PALEONTOLOGY

Disparate compound eyes of Cambrian radiodonts reveal their developmental growth mode and diverse visual ecology

John R. Paterson[1]*, Gregory D. Edgecombe[2], Diego C. García-Bellido[3,4]

Radiodonts are nektonic stem-group euarthropods that played various trophic roles in Paleozoic marine ecosystems, but information on their vision is limited. Optical details exist only in one species from the Cambrian Emu Bay Shale of Australia, here assigned to *Anomalocaris* aff. *canadensis*. We identify another type of radiodont compound eye from this deposit, belonging to '*Anomalocaris*' *briggsi*. This ≤4-cm sessile eye has >13,000 lenses and a dorsally oriented acute zone. In both taxa, lenses were added marginally and increased in size and number throughout development, as in many crown-group euarthropods. Both species' eyes conform to their inferred lifestyles: The macrophagous predator *A.* aff. *canadensis* has acute stalked eyes (>24,000 lenses each) adapted for hunting in well-lit waters, whereas the suspension-feeding '*A.*' *briggsi* could detect plankton in dim down-welling light. Radiodont eyes further demonstrate the group's anatomical and ecological diversity and reinforce the crucial role of vision in early animal ecosystems.

INTRODUCTION

Until recently, *Anomalocaris* and related taxa were typically generalized as large-bodied, raptorial apex predators in Cambrian marine ecosystems (*1*, *2*). United by a pair of spinose, arthropodized frontal appendages, large eyes, a radial oral cone, and a trunk composed of segmental swim flaps, these stem-group euarthropods are collectively known as Radiodonta (*3*). Over the past decade, discovery and documentation of new radiodonts from Cambrian and Early Ordovician Konservat-Lagerstätten globally have changed this picture, as new species have broadened the morphological scope of the group and opened up new interpretations of their ecology. The notion that radiodonts are invariably large bodied is contradicted by essentially complete specimens of, for example, *Lyrarapax* being less than 10 cm in length (*4*–*7*). Nevertheless, gigantism has been upheld for other newly described taxa, with the Early Ordovician *Aegirocassis benmoulai* exceeding 2 m in length (*8*).

Frontal appendages are represented by a variety of new forms, including a few species with elongate ventral endites bearing files of auxiliary spines that confer a sieve-like structure consistent with suspension feeding (*7*–*9*). The spectrum is broadened further by frontal appendages with rake-like endites bearing hooked auxiliary spines that, in concert with carapace morphology, suggest feeding by sediment sifting (*10*).

In parallel with this diversity of food-gathering frontal appendages, the oral cone of radiodonts has been found to display more variability than just the tetraradial, 32-plated form first documented in *Hurdia* and *Peytoia* (*1*). A triradial oral cone, with three rather than four enlarged plates and a variable (rather than fixed) number of small- and intermediate-sized plates, is present in *Anomalocaris* (*11*). There is even variety among tetraradial oral cones, including the presence or absence of features such as stacks of denticulate plates within the mouth opening and nodes on plate surfaces (*12*). Furthermore, new discoveries have revealed accessory feeding structures in certain radiodont lineages. Notably, the family Amplectobeluidae has three pairs of dentate gnathobase-like structures, each pair associated with a segment bearing reduced flaps in the transitional region between the head and the trunk (*13*, *14*).

The radiodont head also features a range of sclerites or carapace elements that have only come to light in the past 15 years (*15*). These include separate dorsal and lateral cephalic plates [as in *Anomalocaris* (*10*, *16*), *Amplectobelua* (*13*), and *Lyrarapax* (*6*)], an integrated carapace composed of dorsal and lateral elements [as in *Hurdia* (*17*)], or in one unusual example, an expanded, horseshoe-shaped carapace [as in *Cambroraster* (*10*, *18*, *19*)].

In contrast to the surge in knowledge of the radiodont head structures listed above, much less is known about the eyes. Although a pair of stalked eyes has been recognized in several different radiodont genera (*1*, *2*, *4*, *6*, *10*, *15*, *16*), only outlines were available until the preserved visual surface was revealed in *Anomalocaris* from the Emu Bay Shale (Cambrian Series 2, Stage 4) of South Australia (*20*). Each stalked eye of *Anomalocaris* is pyriform, with a visual surface showing a huge number of ommatidial lenses arranged with the hexagonal packing typical of euarthropod compound eyes. Examination of new and existing specimens shows that each eye could reach more than 4 cm in length and have >24,000 lenses. This extremely elevated number of ommatidia is consistent with a high measure of acuity expected of a visual predator.

Here, we reinterpret a second type of compound eye from the Emu Bay Shale as belonging to one of the two radiodonts that co-occur in this biota. These isolated eyes were first described (*21*) as that of an unknown arthropod, its visual surface with more than 3000 ommatidia, including a field of enlarged lenses characterized as a "bright zone" (herein referred to as an "acute zone," discussed below). Although *Anomalocaris* was considered as one of the possible taxa to have had these eyes, that assignment was regarded as inconsistent with the expected size of an *Anomalocaris* eye, based on the size of the co-occurring radiodont frontal appendages compared to intact specimens from other deposits. At 7 to 9 mm across their long axis, the eyes are two to three times smaller than expected for adult individuals of Emu Bay Shale *Anomalocaris*. This inconsistency is

[1]Palaeoscience Research Centre, School of Environmental and Rural Science, University of New England, Armidale, NSW 2351, Australia. [2]Department of Earth Sciences, The Natural History Museum, Cromwell Road, London SW7 5BD, UK. [3]School of Biological Sciences, University of Adelaide, Adelaide, SA 5005, Australia. [4]South Australian Museum, North Terrace, Adelaide, SA 5000, Australia.
*Corresponding author. Email: jpater20@une.edu.au

now removed by the discovery of new specimens of the same acute zone–type eye reaching more than 3 cm in diameter.

We argue that these acute zone–type eyes (*21*) are most likely those of '*Anomalocaris' briggsi*, whereas the previously described *Anomalocaris* eyes (*20*) are likely those of *Anomalocaris* aff. *canadensis* (formerly *A.* cf. *canadensis*). Morphological details of the acute zone–type eye suggest that these eyes are not stalked (as previously thought for all radiodonts) (*22*, *23*) but are sessile and accommodated in the head by well-sclerotized cuticular structures. As a result, radiodonts depict a substantially greater disparity in gross eye morphology as well as organization of the visual surface than had been known. This brings the eyes into line with other organ systems in showing morphological and inferred ecological variability across the group. Furthermore, the size range of available material permits insights into the growth mode of eye units, allowing radiodont eyes to be interpreted in the context of euarthropod eye development.

RESULTS

Acute zone–type eyes

The available material shows a considerable size range (Figs. 1 and 2, and table S1) (*21*), with the largest specimen having a preserved long-axis diameter of 30 mm, but its incompleteness makes this an underestimate of actual size (Fig. 2, A to D); comparing the position of the largest lenses to that of complete specimens showing a medial acute zone, we estimate a diameter of 38 mm (after sediment compaction).

Several specimens have an elongate sclerite attached to the assumed dorsoproximal part of the eye that spans most of the width of the visual surface (Figs. 1, D to F, and 2, E to G). This sclerite was previously known only from very incomplete fragments of smooth cuticle and was called a "pedestal" (*21*); it is here referred to as an "eye sclerite." It is bilobate across its distal margin, along which it contacts the visual surface. South Australian Museum (SAM) specimen P54853 preserves only a small fragment of the eye sclerite but has a largely complete distal margin adjoining the visual surface that exactly matches the outline of the eye sclerite, i.e., the dorsomedial projection of the visual surface that is accommodated by the embayment in the eye sclerite (Fig. 1A). The proximal margin of the eye sclerite has a bulge at its mid-length—as seen in the two specimens in which this sclerite is most complete (Figs. 1D and 2G)—that parallels the course of the embayment in its distal margin.

In several specimens, a narrow rim of cuticle (the "marginal rim") completely surrounds the visual surface along the entire extent that is not in contact with the dorsal eye sclerite (Figs. 1, E and F, and 2, E and F), and at least some of the marginal rim is overlapped by the eye sclerite (Fig. 1, E and F). The visual surface is thus entirely surrounded by other cuticular structures (the eye sclerite and marginal rim), indicating that the eyes are sessile and nonstalked, rather than having mobile eye stalks, as previously noted for some radiodonts (*22*).

The medial position of the acute zone—that is, the area displaying the largest lenses—is consistent with previously documented specimens (*21*), with lens diameters gradually decreasing to the margin of the visual surface. New specimens show that especially small lenses are situated along most margins of the visual surface, except in the dorsal region (Figs. 1, A and D, and 2, A to D and G). The entire visual surface exhibits a high degree of ordering of lenses into rows that confer dense hexagonal packing, although regularity is sometimes perturbed by rows coming into irregular contact at a few lenses, even in the acute zone, thus resulting in an imperfect hexagonal pattern in places (Fig. 1, B and C).

No single specimen shows a complete visual surface to enable a precise count of lenses, but across the available sample, the entire preserved surface is covered in lenses. Extrapolating across the best new specimens and inferring comparable size of lenses in the same positions, the number of lenses ranges from c. 5500 in SAM P55428 (total long-axis diameter of 12.2 mm; Fig. 2G) to an estimated c. 13,200 in SAM P57421 (with an extrapolated total long-axis diameter of 28.6 mm; Fig. 1D). Although incomplete, SAM P54248 (Fig. 2, A to D) has an estimated long-axis diameter of 38 mm and similar lens diameters compared with other large specimens (tables S1 and S2), suggesting that the acute zone–type eye may have had well more than 13,000 lenses. These numbers conform to c. 3400 to 4000 lenses in previously known specimens (*21*) with a long-axis diameter of <9 mm. Hence, the overall pattern is that the number of lenses increases as the eye becomes larger (Fig. 3A).

In some of the largest specimens (Figs. 1, A to C, E, and F, and 2, A to D), lens diameters range from c. 260 to 335 μm in the acute zone (Fig. 3B), and then rapidly grade to c. 95 to 170 μm toward the edge of the visual surface, with some of the smallest preserved lenses at the extreme margin being c. 80 μm in diameter (table S1). Smaller eyes have smaller lenses (Fig. 3B); for example, SAM P55428 (with a long-axis diameter of 12.2 mm; Fig. 2G) has lens diameters ranging from c. 175 to 200 μm in the acute zone, down to c. 45 to 65 μm near the margin. This is again consistent with the previously reported lens diameters of small specimens (*21*). Notably, the biggest lenses in the Emu Bay Shale acute zone–type eyes (at 335 μm in diameter) far exceed those of any other Cambrian compound eye, apart from the *Anomalocaris*-type eyes from the Emu Bay Shale described below (*21*, *22*, *24*).

Anomalocaris-type eyes

These eyes (Fig. 4) (*20*) are distinguished from those of acute zone–type eyes by their stalked, more elongate, pyriform shape, and much more consistent lens size across the visual surface. SAM P49070 provides new data on the maximum known size of these eyes, its incomplete visual surface preserving an extent of 38.6 mm along its long axis (Fig. 4A). Lenses measured in a few different areas on this specimen consistently range from c. 295 to 325 μm in diameter. These are larger than the lenses previously reported for SAM P45920 (ranging from c. 70 to 110 μm) (*20*), indicating that, like acute zone–type eyes, lens size increases throughout growth (Fig. 3B).

A previous estimate of c. 16,700 lenses in SAM P45920 was extrapolated from one area with the best-preserved lenses across the entire visual surface (*20*); this was a conservative minimum and certainly an underestimate. Extrapolating average lens counts from 12 separate 1-mm^2 areas distributed across the surface of the better preserved of two eyes in SAM P45920a [figure 1d in (*20*)] yields an estimate of 24,760 lenses on the exposed side of the visual surface (Fig. 3A and table S2); it is likely that the complete three-dimensional visual surface hosted considerably more lenses. In a similar-sized but incomplete specimen (SAM P52893; Fig. 4C), an estimated 16,250 lenses are preserved on the visual surface (table S2).

Association of Emu Bay Shale eyes and radiodont species

Previous concerns about assigning the acute zone–type eye to a radiodont based on irreconcilable differences in size (*21*) can now be dismissed because of the discovery of much larger, appropriate-sized specimens documented here. Accordingly, we now consider a

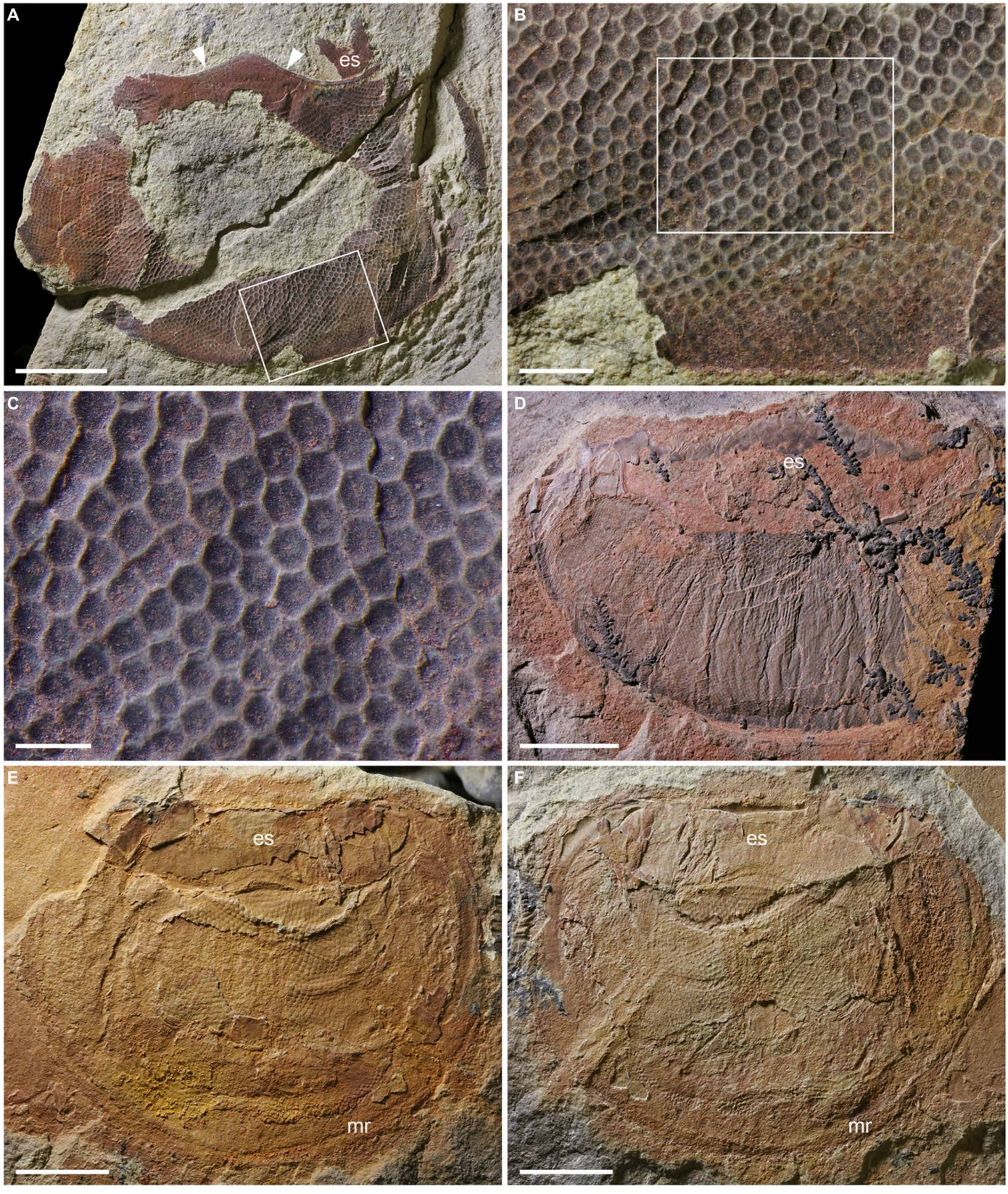

Fig. 1. Acute zone–type eye of *'A.' briggsi*. (**A** to **C**) SAM P54853; inset in (A) shows the position of (B), and inset in (B) shows the position of (C); arrowheads in (A) indicate contact between eye sclerite and visual surface. (**D**) SAM P57421. (**E** and **F**) SAM P48377a,b, part (E) and counterpart (F). Scale bars, 5 mm (A and D to F), 1 mm (B), and 0.5 mm (C). es, eye sclerite; mr, marginal rim. Photo credit: J. Paterson, University of New England (A to F).

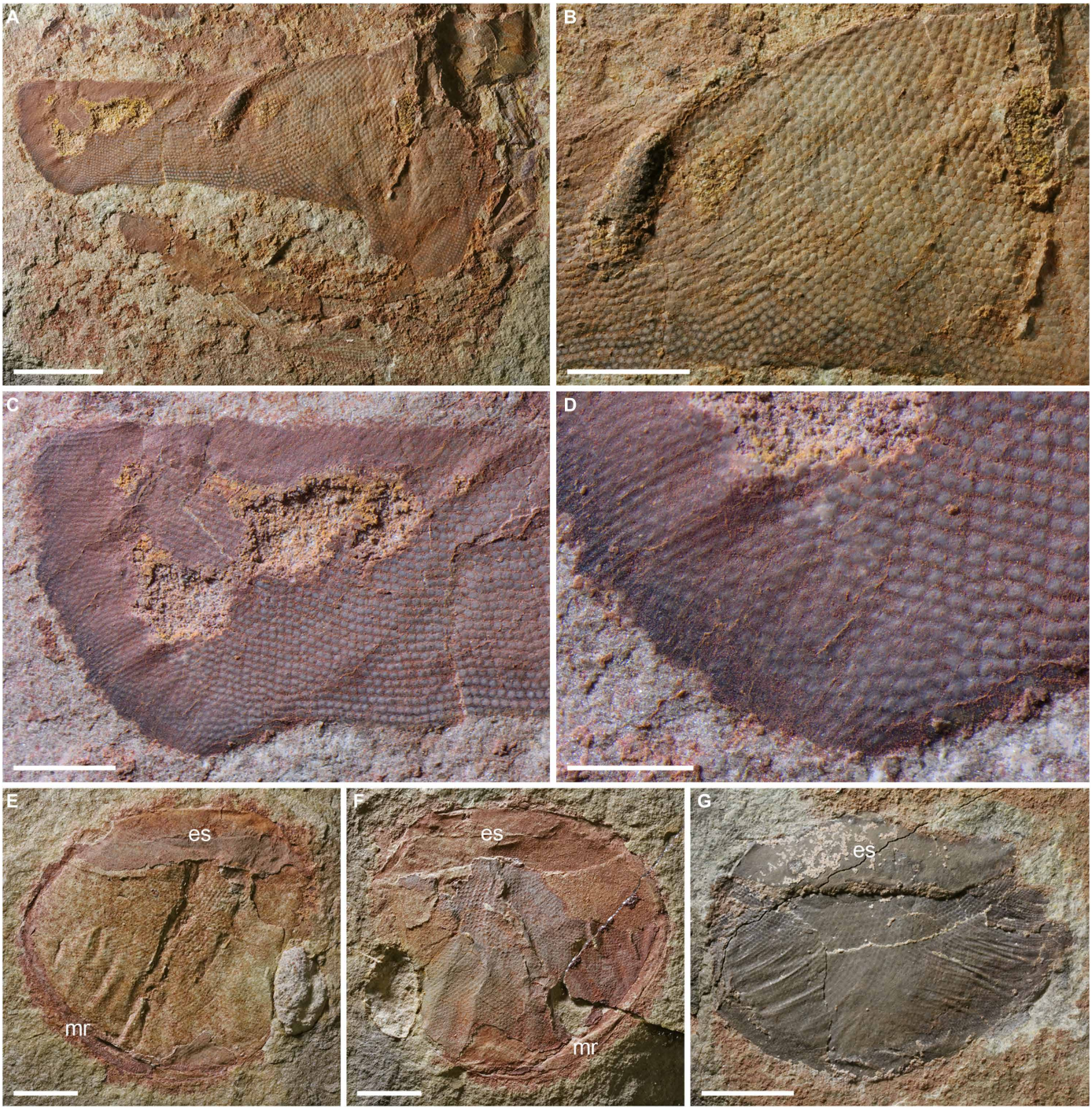

Fig. 2. Acute zone–type eye of *'A.' briggsi*. (**A** to **D**) SAM P54248. (**E** and **F**) SAM P52901a,b, part (E) and counterpart (F). (**G**) SAM P55428. Scale bars, 5 mm (A), 3 mm (B and E to G), 2 mm (C), and 1 mm (D). es, eye sclerite; mr, marginal rim. Photo credit: J. Paterson, University of New England (A to G).

radiodont identity as most reasonable for these eyes, given that no other euarthropods in the Emu Bay Shale approach the body size required to accommodate them. The consistently isolated eye specimens are in accordance with the frequently disarticulated radiodont remains (e.g., frontal appendages, oral cones, and body flaps) from the Emu Bay Shale, resulting from either molting or decay and postmortem disturbance of these more robust, well-sclerotized body parts (*25*). The larger acute zone–type eyes also further weaken the case for assigning them to another possible candidate: the "bivalved" euarthropod, *Tuzoia*. The largest Emu Bay Shale *Tuzoia* specimens with circular eyes preserved in situ show that these visual organs do not reach more than 9 mm in diameter (*21*, *26*), and even the biggest *Tuzoia* carapaces from this deposit would not be able to accommodate acute zone–type eyes more than 3 cm in diameter.

Frontal appendages of '*A.*' *briggsi* and *A.* aff. *canadensis* co-occur throughout the same 1.9-m interval of the Emu Bay Shale at Buck Quarry from which the two types of compound eyes have been collected (tables S3 to S5) (*27*). Among the available frontal appendages from this interval (table S4), '*A.*' *briggsi* is represented by 68 of 81 specimens (~84% of the sample), and *A.* aff. *canadensis* the remaining 13 specimens (~16%); note that a single frontal appendage was counted as one specimen, even if it is preserved as part of an associated pair [e.g., figure 3j in (*25*)]. Correspondingly, acute zone–type eyes represent 21 of the 34 identified eye specimens (~62%), outnumbering those of *Anomalocaris* type (~38%); as with frontal appendages, a single eye was counted as one specimen, even if preserved as one of a pair [e.g., figure 1a in (*20*)]. Thus, in terms of relative abundance, the more common acute zone–type eye most likely belongs to '*A.*' *briggsi*. Also, statistical tests for equality of proportions (table S6) between the frontal appendage and eye types suggest that this association is much more likely than the alternative possibility of the *Anomalocaris*-type eye belonging to '*A.*' *briggsi* (and the acute zone–type eye to *A.* aff. *canadensis*). However, it must be acknowledged that there could be taphonomic inconsistencies in the ratios of preserved frontal appendages and eye types, so these taxonomic associations must be considered tentative based on specimen numbers alone.

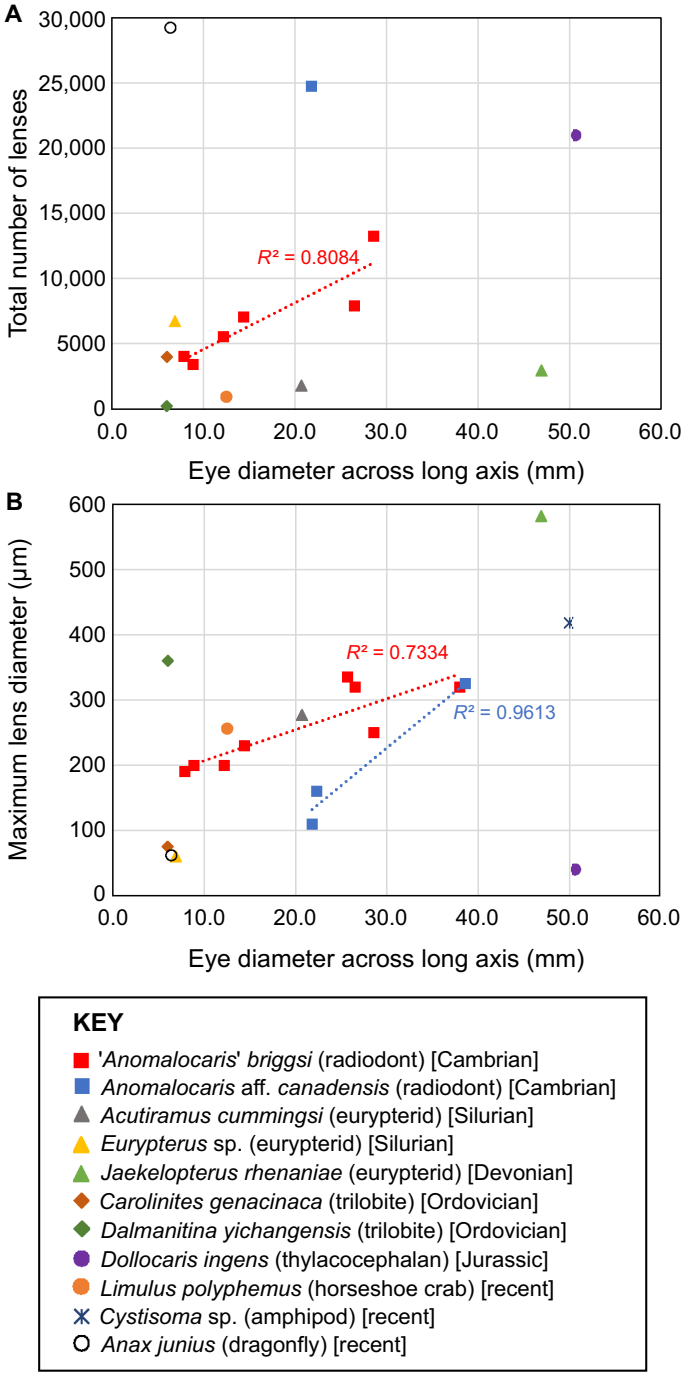

Fig. 3. Eye sizes, lens counts, and lens diameters for the best-preserved Emu Bay Shale radiodont eyes and select euarthropods known for their extreme eye morphology. (**A**) Total number of lenses and (**B**) maximum lens diameter (µm) plotted against maximum eye diameter across long axis (mm). Data sources: *Acutiramus cummingsi* (*34*), *Anax junius* (*39*), '*Anomalocaris*' *briggsi* and *Anomalocaris* aff. *canadensis* (tables S1 and S2), *Carolinites genacinaca* (*21*), *Cystisoma* sp. (*42*), *Dalmanitina yichangensis* (*21*), *Dollocaris ingens* (*37*, *38*), *Eurypterus* sp. (*34*), *Jaekelopterus rhenaniae* (*35*), and *Limulus polyphemus* (*34*).

The relative abundance argument is consistent with the morphological similarities between *Anomalocaris canadensis* from the Burgess Shale (*16*) and *A.* aff. *canadensis* from the Emu Bay Shale (*25*, *27*), especially in their frontal appendages and the tuberculate, triradial oral cone. The pyriform stalked eye from the Emu Bay Shale (Fig. 4) (*20*) more closely resembles that of *A. canadensis* [e.g., figure 1 in (*16*)] than does the sessile acute zone–type eye, providing a solid taxonomic argument for its assignment. Attribution of the acute zone–type eye to '*A.*' *briggsi* thus partly follows from elimination and is congruous with phylogenetic analyses in which '*A.*' *briggsi* is united with *Tamisiocaris*, rather than with Anomalocarididae (*6*–*10*). This phylogenetic relationship is entirely based on frontal appendage characters, and eyes are unknown for *Tamisiocaris*. Nevertheless, affiliation of *A.* aff. *canadensis* and '*A.*' *briggsi* in different parts of the radiodont tree and their classification in different families are compatible with their markedly different eyes. A sessile, nonstalked eye with a small sclerite and cuticular marginal rim now adds another character in which '*A.*' *briggsi* differs substantially from *Anomalocaris*. Hence, we signal this taxonomic uncertainty in referring '*A.*' *briggsi* to *Anomalocaris* with qualification, as noted in recent studies (*7*, *10*).

DISCUSSION

Eye position in the head of '*A.*' *briggsi*

The eye of '*A.*' *briggsi* is argued above to be sessile and nonstalked, the visual surface encircled by the eye sclerite and the marginal rim. We infer that the eye sclerite would be dorsomedial to the visual surface in life, forming a kind of eye covering (similar to the palpebral lobe of trilobites), and the marginal rim would extend along the ventrolateral margin of the eye. As stalked radiodont eyes are situated laterally on the head, we infer the same for the sessile eye of '*A.*' *briggsi* (Fig. 5, A and B).

The eye sclerite of '*A.*' *briggsi* is likely homologous with paired dorsolateral sclerites associated with the stalked eyes of other (nonhurdiid) radiodont taxa. Notably, a juvenile specimen of *Lyrarapax unguispinus* has an anterior dorsomedial head sclerite and a pair of small, elongate lateral sclerites, the latter positioned where the eye stalks originate (*6*). Rather than inferring that the eye sclerite is a wholly novel feature in '*A.*' *briggsi*, it may be more parsimonious to interpret it as a modified version of the lateral sclerite seen in taxa

Fig. 4. Compound eye of *A.* aff. *canadensis*. (**A** and **B**) SAM P49070; inset in (A) shows the position of (B). (**C**) SAM P52893. Scale bars, 5 mm (A and C) and 1 mm (B). Photo credit: J. Paterson, University of New England (A to C).

such as *Lyrarapax*, which is clearly associated with the eye and has a similar shape and orientation (*6*). Some previous studies (*10*, *13*) have inferred homology between the lateral sclerites of certain radiodont genera (e.g., *Amplectobelua* and *Anomalocaris*) and the P-elements of hurdiids. In the latter clade, the P-elements form a complex with the medially situated H-element. A medial head sclerite and paired lateral sclerites occur, for example, in *Amplectobelua symbrachiata* (*13*); in this species, some previously identified eyes (*28*) were reinterpreted as P-elements (*13*). Likewise, in *A. canadensis*, which also has a dorsomedial head sclerite (*16*), structures that had been previously identified as eyes in some specimens were reinterpreted as P-elements (*10*). The case for homology between the eye sclerite of '*A.*' *briggsi* and the lateral sclerites of *L. unguispinus* (and possibly *A. symbrachiata* and *A. canadensis*) is supported by their close association with the eye. However, extending this homology to the P-elements of hurdiids is more problematic, given that the eyes of hurdiids are accommodated by notches in the H-element, rather than being closely associated with the P-elements (*10*, *15*, *17*).

A dorsolateral position of the eye sclerite and the encircling of the visual surface by the marginal rim at the lateral sides of the head would constrain the acute zone to be oriented dorsally. This inferred orientation of the eye differs from that hypothetically used to make an analogy to the eyes of robber flies, in which the acute zone is directed anteriorly [figure 1 in (*21*)].

Development of the visual surface

In the acute zone–type eye of '*A.*' *briggsi*, ordering of lenses into rows involves small marginal lenses grading into the enlarged lenses in the acute zone (Figs. 1, A and B, and 2, A to D). Lenses in the acute zone of some of the biggest specimens are approximately twice as large as those known previously from eyes less than half their size. A maximum diameter of 150 μm was reported in eyes 7 to 9 mm in diameter (*21*) versus 335 μm in large eyes (and consistently in the range of 250 to 330 μm in eyes of diameter greater than 25 mm); intermediate-sized specimens bridge this gap (Fig. 3B). Likewise, in *A.* aff. *canadensis*, the largest new eye specimen (SAM P49070), estimated to be almost twice as long as those previously available (*20*), has much larger lenses (maximum of c. 325 μm versus 110 μm). Therefore, lenses would have continued to increase in size throughout the ontogeny of both radiodont species from the Emu Bay Shale (Fig. 3B). Also, both the largest and smallest lenses are bigger in large eyes relative to small ones, suggesting that the small marginal lenses were the most recently added to the visual surface.

The finding that lenses increase in size and number concurrently with the growth of the eye (Fig. 3) and the likelihood that radiodonts add new ommatidia marginally bring these stem-group euarthropods into line with what has been named the "row-by-row" mode of growth of the compound eye in crown-group euarthropods (*29*). This involves growth of the eye for a considerable duration, or even throughout life, with both a persistent/lifelong proliferation zone at

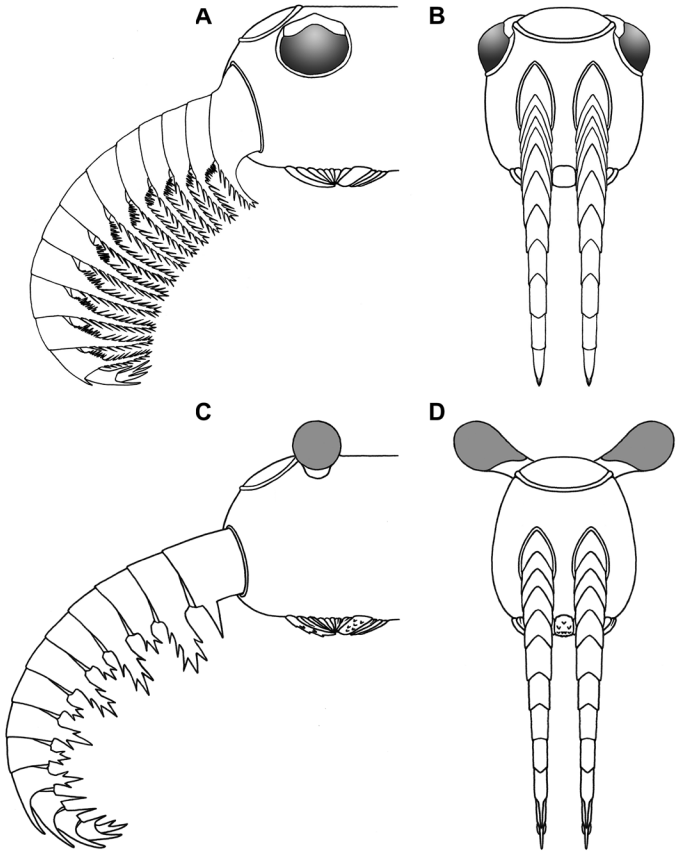

Fig. 5. Head reconstructions of Emu Bay Shale radiodonts, with the visual surface of the eyes shown in gray. (**A** and **B**) *'A.' briggsi* showing sessile (nonstalked) eyes in lateral and anterior views, respectively, with the acute zone depicted by lighter shading; the dorsal head sclerite and oral cone are conjectural. (**C** and **D**) *A.* aff. *canadensis* showing stalked eyes in lateral and anterior views, respectively; the position and orientation of the eyes and the presence of a dorsal head sclerite are based on specimens of *A. canadensis* from the Burgess Shale [e.g., figures 1 and 5 in (*16*); supp. figure 8 in (*10*)] and *Anomalocaris saron* from the Chengjiang biota [e.g., figures 1B and C and 2 in (*2*)], in addition to the eye pair from the Emu Bay Shale [figure 1a and b in (*20*)].

the margin of the visual surface and continuous intercalary growth of ommatidia. This mode of growth is documented in xiphosurans and millipedes (*30*, *31*), as well as in trilobites (*32*), the first two taxa bracketing it as a shared character of Chelicerata and Myriapoda and thus a likely general character for the euarthropod crown group as a whole. This follows from the strong molecular phylogenetic support for a basal split in the euarthropod crown group in which total-group Chelicerata is the sister taxon of Mandibulata, the latter grouping Myriapoda and Pancrustacea together (*33*). The widely endorsed hypothesis that radiodonts are stem-group euarthropods, and indeed branching near the node at which compound eyes originated, means that their mode of growth was conserved across the euarthropod stem-group/crown-group transition. This ancestral pattern was modified in the Pancrustacea, which have a so-called "morphogenetic front type" of eye development in which individual ommatidia, once formed, cease to grow (*29*).

The acute zone–type eye of '*A.*' *briggsi* is noted above to deviate from precise hexagonal packing of its ommatidia by sporadic irregularity in rows. However, across the visual surface and especially in or near the acute zone, the hexagonal arrangement of neighboring ommatidia is more precise than observed in the xiphosuran *Limulus polyphemus*, which shows about one-third of all ommatidia as having more or fewer neighbors than predicted by a hexagonal model (*30*).

Functional morphology and ecology

The compound eyes of radiodonts are outliers among Cambrian euarthropods given their massive size, abundant ommatidia, and huge lens diameters. Across the entire euarthropod fossil record, only giant eurypterids (*34*–*36*) and thylacocephalans (*37*, *38*) have larger eyes (Fig. 3). A single eye of *A.* aff. *canadensis* with more than 24,000 lenses is rivaled only by certain predatory insects such as dragonflies (Fig. 3A) (*39*, *40*), and the enormous lens diameters of '*A.*' *briggsi* (up to 335 μm) are matched only by select marine euarthropods, such as some phacopine trilobites (*21*, *41*), Siluro-Devonian pterygotid eurypterids (*35*), and some modern deep-sea amphipod crustaceans (Fig. 3B) (*42*). A large visual field in radiodonts may be associated with both increased lens number and lens diameter, and a positive correlation of each of these with body size in species of *Drosophila* (*43*) is broadly (if inconsistently) applicable for compound eyes in other euarthropods (*44*–*50*). The exceptional features of radiodont eyes are thus, to some extent, probably consequences of large body size.

The previously documented eyes of '*A.*' *briggsi*, although small, clearly show a distinct region of enlarged lenses that was originally interpreted as an anteriorly directed "bright zone"—an area of high visual acuity and light sensitivity (*21*). In the compound eyes of some insects, such as male blowflies and hoverflies, the large lenses in the bright zone allow for increased light capture but maintain a similar spatial resolution compared with other parts of the visual surface (*51*, *52*). This contrasts with many other terrestrial and marine euarthropod eyes, where the large lenses within the "acute zone" typically have high resolving power and enhanced light capture, but usually at the expense of lower resolution and sensitivity in areas with smaller lenses (*40*, *53*, *54*). Because of the compressed and distorted visual surface, plus the absence of internal ommatidial structures in eye specimens of '*A.*' *briggsi*, the degree of acuity and sensitivity cannot be determined, so we use the broader term "acute zone."

Reinterpretation of the '*A.*' *briggsi* sessile eye (Fig. 5, A and B) as having a dorsally oriented acute zone with huge lenses has important implications regarding the habitat and visual capabilities of this species. As noted above, a considerable diversity of modern euarthropods has acute zones, from terrestrial insects to deep-sea crustaceans (*40*). Of particular relevance here are hyperiid amphipods that inhabit a vast range of ocean depths, chiefly within the epipelagic and mesopelagic zones (down to 1000 m), and show considerable variety in sessile eye morphologies (*42*, *55*). The visual ecology of hyperiids has been well studied (*42*, *55*–*57*) and provides a useful analog for understanding the functional morphology of the '*A.*' *briggsi* eye.

The apposition compound eyes of hyperiid amphipods exhibit some interesting morphological trends with respect to water depth, reflecting adaptations to the directionality and intensity of available light. In general, as water depth increases and light becomes dimmer, bluer, and more vertically down-welling (i.e., progressively point-like) (*58*), the eyes become larger and bilobed, with the dorsal lobe having more numerous and enlarged lenses

(forming an acute zone with a narrow visual field), resulting in enhanced resolution and photon capture (*42*, *57*). In *Cystisoma*, one of the largest and deepest-living hyperiids, only the dorsal lobes are present, with some of the largest individuals (body length, ca. 170 mm) having an enormous visual surface that covers the majority of the head (dorsal exsagittal length, up to 50 mm) and can have huge lenses (>400 μm in diameter) (Fig. 3B) (*42*, *56*). The dorsally biased optics of deep-sea hyperiids permit them to detect small objects silhouetted against the dim down-welling light from above (*54*, *55*, *57*).

The similar eye morphology of '*A.*' *briggsi*—particularly the overall size (<40 mm) and dorsally directed acute zone with massive (≤335-μm diameter) lenses—is suggestive of this radiodont being a mesopelagic species, capable of inhabiting depths of several hundred meters; despite the Emu Bay Shale Konservat-Lagerstätte being deposited nearshore, the biota was buried in a prodelta setting of a localized, tectonically active, deep-water marine basin (*25*, *59*). In the clearest modern oceans, light intensity is reduced by 1.5 orders of magnitude for every 100 m of depth (*58*) and also varies markedly in a 24-hour cycle, regardless of photic zone depth (*54*). Like many deep-sea animals, it is possible that '*A.*' *briggsi* made daily vertical migrations to ensure an environment with relatively constant ambient light levels, which may have also coincided with feeding. Notably, '*A.*' *briggsi* is an inferred microphagous suspension feeder (*7*, *9*), and so probably used its acute, light-sensitive eyes to detect mesoplanktonic organisms (up to 20 mm in size), especially large-scale swarms, at greater depths during the day and/or in the shallower waters during twilight hours.

The highly acute eyes of *A.* aff. *canadensis* from the Emu Bay Shale biota (Fig. 5, C and D) are clearly adapted for hunting in relatively well-lit waters. This is supported by the extremely high number of lenses in each eye (>24,000), as well as previously estimated values of the interommatidial angle (<1.4°) and eye parameter (<2) (*20*). New specimens showing larger lens diameters (≤325 μm) suggest that perhaps *A.* aff. *canadensis* eyes were also capable of functioning in slightly dimmer light. However, similar-sized lenses across an extensive visual field indicate that the eyes were more attuned to operating in the scattered (nondirectional) and extended space light of shallower waters (*58*). Such vision would have allowed this macrophagous predator to detect potential prey in both the water column and on the illuminated seafloor.

The disparate and complex eyes of radiodonts echo other recent discoveries showing that the morphology of this group is far more diverse than previously appreciated, especially with regard to their feeding structures and inferred diets. This diversity now extends to their visual ecology, reinforcing the notion that vision played a crucial role in the evolution of early animal ecosystems (*60*, *61*) and exemplifies the rapid speed at which anatomical innovations took place during the early Cambrian (*21*, *24*, *62*).

MATERIALS AND METHODS

Fossil material

The eyes described herein were collected from a 1.9-m interval of the Emu Bay Shale within Buck Quarry (levels 9.8 to 11.7 m), Kangaroo Island, South Australia (*25*). The seven specimens of acute zone–type eyes previously known (*21*) are supplemented by an additional 14 specimens collected since 2012. Three previously known *Anomalocaris*-type eyes (two of them an associated pair) (*20*) are supplemented by 10 new specimens. All specimens are registered in the South Australian Museum Palaeontology collection, Adelaide (SAM P registration numbers; table S3).

Fossil analyses

Some specimens were mechanically prepared using a pneumatic percussion needle to remove matrix covering the fossil. All specimens were photographed using a Canon EOS 5Ds digital SLR camera with a Canon MP-E 65-mm macro lens, a Cognisys StackShot 3X stacking system, and the Canon EOS Utility software. Close-up images and ommatidial lens diameter measurements (table S1) were obtained with an Olympus SZX7 binocular microscope with an Olympus SC50 camera attachment and the Olympus cellSens Standard v.1.17 software. All images were stacked using the Helicon Focus v.7.5.4 Pro software.

Lenses were counted on high-resolution images of the eyes using Photoshop CS3. On acute zone–type eyes, acute, intermediate, and marginal zones were defined (each approximately one-third of the total visual surface, their boundaries being gradational), on which repeated counts along lens rows were carried out (133 to 440 lenses per specimen). The obtained number of lenses per millimeter in each zone was squared and extrapolated to the total surface of that zone, and the three estimates were added to produce a total lens count for each eye. On *Anomalocaris*-type eyes, rows of as many ommatidia as possible were counted on each visual surface (150 to 300 lenses per specimen) to obtain the number of lenses per millimeter, which was squared and extrapolated to the total preserved visual surface. All these counts can be accessed in tables S1 and S2.

SUPPLEMENTARY MATERIALS

Supplementary material for this article is available at http://advances.sciencemag.org/cgi/content/full/6/49/eabc6721/DC1

View/request a protocol for this paper from *Bio-protocol*.

REFERENCES AND NOTES

1. H. B. Whittington, D. E. G. Briggs, The largest Cambrian animal, *Anomalocaris*, Burgess Shale, British Columbia. *Phil. Trans. R. Soc.* **309**, 569–609 (1985).
2. J. Chen, L. Ramsköld, G. Zhou, Evidence for monophyly and arthropod affinity of Cambrian giant predators. *Science* **264**, 1304–1308 (1994).
3. D. Collins, The "evolution" of *Anomalocaris* and its classification in the arthropod class Dinocarida (nov.) and order Radiodonta (nov.). *J. Paleo.* **70**, 280–293 (1996).
4. P. Cong, X. Ma, X. Hou, G. D. Edgecombe, N. J. Strausfeld, Brain structure resolves the segmental affinity of anomalocaridid appendages. *Nature* **513**, 538–542 (2014).
5. P. Cong, A. C. Daley, G. D. Edgecombe, X. Hou, A. Chen, Morphology of the radiodontan *Lyrarapax* from the early Cambrian Chengjiang biota. *J. Paleo.* **90**, 663–671 (2016).
6. J. Liu, R. Lerosey-Aubril, M. Steiner, J. A. Dunlop, D. Shu, J. R. Paterson, Origin of raptorial feeding in juvenile euarthropods revealed by a Cambrian radiodontan. *Nat. Sci. Rev.* **5**, 863–869 (2018).
7. R. Lerosey-Aubril, S. Pates, New suspension-feeding radiodont suggests evolution of microplanktivory in Cambrian macronekton. *Nat. Commun.* **9**, 3774 (2018).
8. P. Van Roy, A. C. Daley, D. E. G. Briggs, Anomalocaridid trunk limb homology revealed by a giant filter-feeder with paired flaps. *Nature* **522**, 77–80 (2015).
9. J. Vinther, M. Stein, N. R. Longrich, D. A. T. Harper, A suspension-feeding anomalocarid from the Early Cambrian. *Nature* **507**, 496–499 (2014).
10. J. Moysiuk, J.-B. Caron, A new hurdiid radiodont from the Burgess Shale evinces the exploitation of Cambrian infaunal food sources. *Proc. Biol. Sci.* **286**, 20191079 (2019).
11. A. C. Daley, J. Bergström, The oral cone of *Anomalocaris* is not a classic "peytoia". *Naturwissenschaften* **99**, 501–504 (2012).
12. H. Zeng, F. Zhao, Z. Yin, M. Zhu, A new radiodontan oral cone with a unique combination of anatomical features from the early Cambrian Guanshan Lagerstätte, eastern Yunnan, South China. *J. Paleontol.* **92**, 40–48 (2018).

13. P. Cong, A. C. Daley, G. D. Edgecombe, X. Hou, The functional head of the Cambrian radiodontan (stem-group Euarthropoda) *Amplectobelua symbrachiata*. *BMC Evol. Biol.* **17**, 208 (2017).
14. P.-Y. Cong, G. D. Edgecombe, A. C. Daley, J. Guo, S. Pates, X.-G. Hou, New radiodonts with gnathobase-like structures from the Cambrian Chengjiang biota and implications for the systematics of Radiodonta. *Pap. Palaeontol.* **4**, 605–621 (2018).
15. A. C. Daley, G. E. Budd, J.-B. Caron, G. D. Edgecombe, D. Collins, The Burgess Shale anomalocaridid *Hurdia* and its significance for early euarthropod evolution. *Science* **323**, 1597–1600 (2009).
16. A. C. Daley, G. D. Edgecombe, Morphology of *Anomalocaris canadensis* from the Burgess Shale. *J. Paleo.* **88**, 68–91 (2014).
17. A. C. Daley, G. E. Budd, J.-B. Caron, Morphology and systematics of the anomalocaridid arthropod *Hurdia* from the Middle Cambrian of British Columbia and Utah. *J. Syst. Palaeontol.* **11**, 743–787 (2013).
18. Y. Liu, R. Lerosey-Aubril, D. Audo, D. Zhai, H. Mai, J. Ortega-Hernández, Occurrence of the eudemersal radiodont *Cambroraster* in the early Cambrian Chengjiang Lagerstätte and the diversity of hurdiid ecomorphotypes. *Geol. Mag.* **157**, 1200–1206 (2020).
19. Z. Sun, H. Zeng, F. Zhao, Occurrence of the hurdiid radiodont *Cambroraster* in the middle Cambrian (Wuliuan) Mantou Formation of North China. *J. Paleo.* **94**, 881–886 (2020).
20. J. R. Paterson, D. C. García-Bellido, M. S. Y. Lee, G. A. Brock, J. B. Jago, G. D. Edgecombe, Acute vision in the giant Cambrian predator *Anomalocaris* and the origin of compound eyes. *Nature* **480**, 237–240 (2011).
21. M. S. Y. Lee, J. B. Jago, D. C. García-Bellido, G. D. Edgecombe, J. G. Gehling, J. R. Paterson, Modern optics in exceptionally preserved eyes of Early Cambrian arthropods from Australia. *Nature* **474**, 631–634 (2011).
22. N. J. Strausfeld, X. Ma, G. D. Edgecombe, R. A. Fortey, M. F. Land, Y. Liu, P. Cong, X. Hou, Arthropod eyes: The early Cambrian fossil record and divergent evolution of visual systems. *Arthropod Struct. Dev.* **45**, 152–172 (2016).
23. T.-Y. Park, J.-H. Kihm, J. Woo, C. Park, W. Y. Lee, M. P. Smith, D. A. T. Harper, F. Young, A. T. Nielsen, J. Vinther, Brain and eyes of *Kerygmachela* reveal protocerebral ancestry of the panarthropod head. *Nat. Commun.* **9**, 1019 (2018).
24. F. Zhao, D. J. Bottjer, S. Hu, Z. Yin, M. Zhu, Complexity and diversity of eyes in Early Cambrian ecosystems. *Sci. Rep.* **3**, 2751 (2013).
25. J. R. Paterson, D. C. García-Bellido, J. B. Jago, J. G. Gehling, M. S. Y. Lee, G. D. Edgecombe, The Emu Bay Shale Konservat-Lagerstätte: A view of Cambrian life from East Gondwana. *J. Geol. Soc. Lond.* **173**, 1–11 (2016).
26. D. C. García-Bellido, J. R. Paterson, G. D. Edgecombe, J. B. Jago, J. G. Gehling, M. S. Y. Lee, The bivalved arthropods *Isoxys* and *Tuzoia* with soft-part preservation from the lower Cambrian Emu Bay Shale Lagerstätte (Kangaroo Island, Australia). *Palaeontology* **52**, 1221–1241 (2009).
27. A. C. Daley, J. R. Paterson, G. D. Edgecombe, D. C. García-Bellido, J. B. Jago, New anatomical information on *Anomalocaris* from the Cambrian Emu Bay Shale of South Australia and a reassessment of its inferred predatory habits. *Palaeontology* **56**, 971–990 (2013).
28. X. Hou, J. Bergström, P. Ahlberg, *Anomalocaris* and other large animals in the Lower Cambrian Chengjiang fauna of southwest China. *GFF* **117**, 163–183 (1995).
29. S. Harzsch, G. Hafner, Evolution of eye development in arthropods: Phylogenetic aspects. *Arthropod Struct. Dev.* **35**, 319–340 (2006).
30. S. Harzsch, K. Vilpoux, D. C. Blackburn, D. Platchetzki, N. L. Brown, R. Melzer, K. E. Kempler, B. A. Battelle, Evolution of arthropod visual systems: Development of the eyes and central visual pathways in the horseshoe crab *Limulus polyphemus* Linnaeus, 1758 (Chelicerata, Xiphosura). *Dev. Dyn.* **235**, 2641–2655 (2006).
31. S. Harzsch, R. R. Melzer, C. H. G. Müller, Mechanisms of eye development and evolution of the arthropod visual system: The lateral eyes of Myriapoda are not modified insect ommatidia. *Org. Divers. Evol.* **7**, 20–32 (2007).
32. A. T. Thomas, Developmental palaeobiology of trilobite eyes and its evolutionary significance. *Earth Sci. Rev.* **71**, 77–93 (2005).
33. G. Giribet, G. D. Edgecombe, The phylogeny and evolutionary history of arthropods. *Curr. Biol.* **29**, R592–R602 (2019).
34. R. P. Anderson, V. E. McCoy, M. E. McNamara, D. E. G. Briggs, What big eyes you have: The ecological role of giant pterygotid eurypterids. *Biol. Lett.* **10**, 20140412 (2014).
35. V. E. McCoy, J. C. Lamsdell, M. Poschmann, R. P. Anderson, D. E. G. Briggs, All the better to see you with: Eyes and claws reveal the evolution of divergent ecological roles in giant pterygotid eurypterids. *Biol. Lett.* **11**, 20150564 (2015).
36. M. Poschmann, B. Schoenemann, V. E. McCoy, Telltale eyes: The lateral visual systems of Rhenish Lower Devonian eurypterids (Arthropoda, Chelicerata) and their palaeobiological implications. *Palaeontology* **59**, 295–304 (2016).
37. S. Charbonnier, J. Vannier, P. Hantzpergue, C. Gaillard, Ecological significance of the arthropod fauna from the Jurassic (Callovian) La Voulte Lagerstätte. *Acta Palaeontol. Pol.* **55**, 111–132 (2010).
38. J. Vannier, B. Schoenemann, T. Gillot, S. Charbonnier, E. Clarkson, Exceptional preservation of eye structure in arthropod visual predators from the Middle Jurassic. *Nat. Commun.* **7**, 10320 (2016).
39. T. E. Sherk, Development of the compound eyes of dragonflies (Odonata). III. Adult compound eyes. *J. Exp. Zool.* **203**, 61–80 (1978).
40. M. F. Land, D.-E. Nilsson, *Animal Eyes* (Oxford Univ. Press, ed. 2, 2012), pp. 271.
41. B. Schoenemann, E. N. K. Clarkson, Vision in fossilised eyes. *Earth Environ. Sci. Trans. R. Soc. Edinb.* **106**, 209–220 (2017).
42. M. F. Land, The eyes of hyperiid amphipods: Relations of optical structure to depth. *J. Comp. Physiol. A* **164**, 751–762 (1989).
43. N. Posnien, C. Hopfen, M. Hilbrant, M. Ramos-Womack, S. Murat, A. Schönauer, S. L. Herbert, M. D. D. Nunes, S. Arif, C. J. Breuker, C. Schlötterer, P. Mitteroecker, A. P. McGregor, Evolution of eye morphology and Rhodopsin expression in the *Drosophila melanogaster* species subgroup. *PLOS ONE* **7**, e37346 (2012).
44. P. Hiller-Adams, J. F. Case, Optical parameters of euphausiid eyes as a function of habitat depth. *J. Comp. Physiol. A* **154**, 307–318 (1984).
45. P. Hiller-Adams, J. F. Case, Optical parameters of the eyes of some benthic decapods as a function of habitat depth (Crustacea, Decapoda). *Zoomorphology* **105**, 108–113 (1985).
46. P. Hiller-Adams, J. F. Case, Eye size of pelagic crustaceans as a function of habitat depth and possession of photophores. *Vision Res.* **28**, 667–680 (1988).
47. V. B. Meyer-Rochow, D. Towers, I. Ziedins, Growth patterns in the eye of *Petrolisthes elongatus* (Crustacea; Decapoda; Anomura). *Exp. Biol.* **48**, 329–340 (1990).
48. T. Bauer, M. Kredler, Morphology of the compound eyes as an indicator of life-style in carabid beetles. *Can. J. Zool.* **71**, 799–810 (1993).
49. E. Keskinen, Y. Takaku, V. B. Meyer-Rochow, T. Hariyama, Postembryonic eye growth in the seashore isopod *Ligia exotica* (Crustacea, Isopoda). *Biol. Bull.* **202**, 223–231 (2002).
50. R. L. Rutowski, L. Gislén, E. J. Warrant, Visual acuity and sensitivity increase allometrically with body size in butterflies. *Arthropod Struct. Dev.* **38**, 91–100 (2009).
51. J. H. van Hateren, R. C. Hardie, A. Rudolph, S. B. Laughlin, D. G. Stavenga, The bright zone, a specialized dorsal eye region in the male blowfly *Chrysomyia megacephala*. *J. Comp. Physiol. A* **164**, 297–308 (1989).
52. A. D. Straw, E. J. Warrant, D. C. O'Carroll, A 'bright zone' in male hoverfly (*Eristalis tenax*) eyes and associated faster motion detection and increased contrast sensitivity. *J. Exp. Biol.* **209**, 4339–4354 (2006).
53. M. F. Land, *Adaptive Mechanisms in the Ecology of Vision* (Kluwer, 1999), pp. 51–71.
54. E. J. Warrant, *Ecology of Sensing* (Springer-Verlag, 2001), pp. 187–213.
55. J. L. Baldwin Fergus, S. Johnsen, K. J. Osborn, A unique apposition compound eye in the mesopelagic hyperiid amphipod *Paraphronima gracilis*. *Curr. Biol.* **25**, 473–478 (2015).
56. M. F. Land, Optics of the eyes of *Phronima* and other deep-sea amphipods. *J. Comp. Physiol. A* **145**, 209–226 (1981).
57. M. F. Land, On the functions of double eyes in midwater animals. *Philos. Trans. R. Soc. Lond. B* **355**, 1147–1150 (2000).
58. E. J. Warrant, N. A. Locket, Vision in the deep sea. *Biol. Rev. Camb. Philos. Soc.* **79**, 671–712 (2004).
59. J. G. Gehling, J. B. Jago, J. R. Paterson, D. C. García-Bellido, G. D. Edgecombe, The geological context of the Lower Cambrian (Series 2) Emu Bay Shale Lagerstätte and adjacent stratigraphic units, Kangaroo Island, South Australia. *Aust. J. Earth Sci.* **58**, 243–257 (2011).
60. R. E. Plotnick, S. Q. Dornbos, J. Chen, Information landscapes and sensory ecology of the Cambrian radiation. *Paleobiology* **36**, 303–317 (2010).
61. A. R. Parker, On the origin of optics. *Opt. Laser Technol.* **43**, 323–329 (2011).
62. J. R. Paterson, G. D. Edgecombe, M. S. Y. Lee, Trilobite evolutionary rates constrain the duration of the Cambrian explosion. *Proc. Natl. Acad. Sci. U.S.A.* **116**, 4394–4399 (2019).

Acknowledgments: We thank our previous collaborators on Emu Bay Shale research, J. Gehling, J. Jago, and M. Lee, as well as R. Atkinson, M. Betts, R. Bicknell, M.-A. Binnie, G. Brock, A. Camens, A. Daley, H. Drage, E. Ellis, R. Gaines, M. Gemmell, J. Holmes, T. and C. Ireland, K. Kenny, P. Kruse, J. Laurie, B. McHenry, M. Mills, J. Ortega-Hernández, L. Reid, D. Rice, and N. Schroeder for assisting with collecting efforts. J. Holmes, R. Bicknell, and N. Campione provided useful discussions and assistance on statistical tests, and M. Tighe and M. White generously helped with exploring various imaging techniques. Financial and logistical assistance was provided by the South Australian Museum and SeaLink. Last, thanks to landowners P. and C. Buck for generously allowing access to the field site. **Funding:** This research was supported by grants from the Australian Research Council, including Future Fellowships (FT120100770 to J.R.P. and FT130101329 to D.C.G.-B.) and a Discovery Project (DP200102005 to J.R.P. and G.D.E.). **Author contributions:** J.R.P. conceived the study. J.R.P. and G.D.E. conducted the photography and wrote the first draft of the manuscript with subsequent input from D.C.G.-B.; D.C.G.-B. carried out the

ommatidial counts, obtained total lens estimates, and produced the head reconstructions with input from J.R.P. and G.D.E.; J.R.P. and D.C.G.-B. drafted the figures with input from G.D.E.; and all authors analyzed and interpreted the fossil material, contributed to discussions, and edited and approved the final manuscript. **Competing interests:** The authors declare that they have no competing interests. **Data and materials availability:** All data needed to evaluate the conclusions in the paper are present in the paper and/or the Supplementary Materials. Additional data related to this paper may be requested from the authors.

Submitted 7 May 2020
Accepted 20 October 2020
Published 2 December 2020
10.1126/sciadv.abc6721

Citation: J. R. Paterson, G. D. Edgecombe, D. C. García-Bellido, Disparate compound eyes of Cambrian radiodonts reveal their developmental growth mode and diverse visual ecology. *Sci. Adv.* **6**, eabc6721 (2020).